AIAA 79-1689R

Subsonic Free-Flight Data for a Complex Asymmetric Missile

Robert H. Whyte*
General Electric Co., Burlington, Vt.
Gerald L. Winchenbach†
Air Force Armament Laboratory, Eglin Air Force Base, Fla.
and
Wayne H. Hathaway‡
General Electric Co., Burlington, Vt.

A systematic technique used to extract the asymmetric aerodynamics from the measured motion patterns of complex missile configurations has been demonstrated. This paper discusses this technique which utilizes the maximum likelihood method, the equations of motion used in the reduction routines, and presents asymmetric aerodynamic derivatives and coefficients obtained from ballistic range tests of a typical complex missile configuration. These data show that the current state-of-the-art in free-flight testing is such that neither mathematical complexity nor computational difficulties represent serious limitations upon what can be successfully tested and analyzed within the ballistic range.

Nomenclature

A = reference area $= \pi d^2/4$
a_c = Coriolis acceleration
C_l = roll moment coefficient
C_{lp} = roll damping coefficient
C_{l_γ} = induced roll moment coefficient
$C_{l_\delta}\delta$ = roll moment due to fin cant
C_m = pitch moment coefficient
C_{m_γ} = induced pitching moment coefficient
C_{mq} = damping-in-pitch coefficient
C_n = side moment coefficient
C_{n_γ} = induced side moment coefficient
C_{nr} = damping-in-yaw coefficient
C_X = axial force coefficient
C_Y = side force coefficient
C_{Yp} = magnus force coefficient
C_{Y_γ} = induced side force coefficient
C_Z = pitch force coefficient
C_{Z_γ} = induced pitch force coefficient
d = reference diameter
F_{xb}, F_{yb}, F_{zb} = force components
g = gravity
I_x, I_y, I_z = moments of inertia
l = model length
L_b, M_b, N_b = moment components
m = mass
M = Mach number
N = number of fins (2 for present configuration)
p_b, q_b, r_b = body-fixed angular velocities
q = dynamic pressure
u_v, v_b, w_b = body-fixed velocity components
V = total velocity
x, y, z = missile Earth-fixed coordinates
$X_{c.g.}/l$ = center of gravity
α = pitch angle, w_b/V
$\bar{\alpha}$ = total angle of attack
β = yaw angle, v_b/V
ϵ = sine of the total angle of attack $= \left[\frac{v_b^2 + w_b^2}{V}\right]^{1/2}$
γ = aerodynamic roll angle
θ, ψ, ϕ = rotation angles

Superscripts

$(\dot{})$ = first derivative with respect to time
$(\bar{})$ = total values

Subscripts

$\bar{\alpha}$ = derivative with respect to ϵ
$\bar{\alpha}_2$ = derivative with respect to ϵ^2
$\bar{\alpha}_i$ = derivative with respect to ϵ^i
α = derivative with respect to α
β = derivative with respect to β

Introduction

HISTORICALLY, free-flight testing in ballistic ranges has been limited to relatively simple aerodynamic configurations. This restriction was caused not by an inability to launch and measure the associated position-attitude time histories of complex asymmetric missile configurations, but by the lack of a systematic technique to extract the asymmetric aerodynamics from the measured motion patterns. Prior to 1969, the most prevalent method of analyzing ballistic spark range data was based on the linear approximation known as "linear theory" developed by Murphy,[1-3] MacAllister,[4,5] Nicolaides,[5-7] Eikenberry,[8] and others. Stated briefly, the method used a closed-form approximate solution to the differential equations of motion. This approximate solution asssumed not only a linearized aerodynamic model, but small aerodynamic asymmetries and at least two planes of identical mass symmetry. These assumptions eliminated the class of model configurations possessing only one plane of symmetry from testing and analysis in free-flight ballistic ranges.

In 1969 Chapman and Kirk of NASA Ames, in analyzing free-flight data,[9] documented the application of a technique which permitted the free-flight differential equations of motion to be used directly in the data correlation process.

Presented as Paper 79-1689 at the AIAA Atmospheric Flight Mechanics Conference, Boulder, Colo., Aug. 6-8, 1979; submitted Nov. 5, 1979; revision received May 9, 1980.

*Advanced Design Engineer, Armament Systems Department. Member AIAA.
†Project Engineer, Gun, Rockets and Explosives Division. Member AIAA.
‡Advanced Design Engineer, Armament Systems Department.

This technique eliminated the requirement for closed-form approximations to the equations of motion and the resulting symmetry assumptions. As applied, the only limitation of this technique was that the translational and angular motion of the test items were sufficiently independent, such that decoupling of the two modes was permissible. However, when considering highly complex aerodynamic configurations possessing wings, etc., large normal forces can be expected and the limitation that decoupling imposes appears unnecessarily restrictive.

Recently, the maximum likelihood method, a technique used for determining aircraft stability and control parameters from data acquired using onboard telemetry, has been applied to the free-flight data analysis problem of missile configurations.[10] This method provides the capability for the simultaneous correlation of the translational and angular motion data, thus eliminating the remaining restrictions on the equations of motion. Theoretically, the aerodynamic coefficients of any test configuration regardless of complexity can be determined within the limits of coefficient accuracy dictated by the raw data accuracy and provided that the aerodynamic model used is functionally adequate. Therefore, this effort was initiated to develop and demonstrate the technique of extracting the asymmetric aerodynamics of a complex missile configuration from the measured free-flight motions.

This paper discusses the maximum likelihood method as applied to ballistic range data analysis, the equations of motion, and the functional forms of the aerodynamic model used within the reduction routines, and presents the asymmetric aerodynamic derivatives and coefficients obtained from tests of a complex missile configuration. A brief description of the missile configuration and the testing techniques is also presented.

Test Facility and Free-Flight Models

Test Facility

The tests were conducted in the Aeroballistic Research Facility at the Air Force Armament Laboratory. This facility is an enclosed, atmospheric, instrumented, concrete structure used to examine the exterior ballistics of various free-flight munitions. The 207-m instrumented length of the range has a 3.66×3.66 m cross section for the first 69 m and a 4.88×4.88 m cross section for the remaining length. The range has 131 instrumentation site locations. Each location has a physical separation of 1.5 m and 50 of the sites are presently used to house fully instrumented orthogonal shadowgraph stations. For the present tests the flights were purposely terminated about one-third of the distance downrange because of the expected large dispersions caused by the model's lift. The nominal operating temperature of the range is 22°C. A complete description of the Aeroballistic Research Facility appears in Ref. 11.

Free-Flight Models

The model configuration chosen to demonstrate the analysis technique is shown in Figs. 1 and 2. This configuration was chosen for three reasons: 1) the availability of the models, 2) the highly asymmetric nature of the configuration, and 3) the present interest in "cruise-type" missile configurations. The models were flown at ground level atmospheric pressure conditions and a subsonic Mach number of about 0.63. The physical properties of the three models which were used to demonstrate the data analysis technique are tabulated in Table 1.

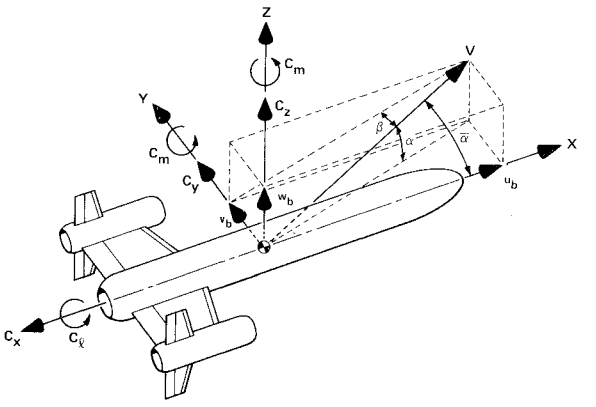

Fig. 1 Definition of body-fixed coordinate system.

The models were launched from a 15.25 cm i.d. compressed-air launcher using four-component sabots which were aerodynamically separated during launch. The models were not canted with respect to the sabot; therefore, the initial disturbances associated with the normal model-sabot separation process provided the motion obtained during flight. A photograph of the model-sabot package is shown in Fig. 3.

Initially, it was hoped that additional models possessing canards could be flown and the resulting motion patterns also analyzed. One of these models was used for the photograph of Fig. 3. However, when ballasting these models in order to obtain the desired center-of-gravity location, the destabilizing effects of the canards were underestimated. This resulted in a near neutrally stable configuration. Three of these models were actually flown, but resulted in short and erratic flights and, subsequently, were not usable in the data analysis scheme as too few valid data points were obtained. Figure 4 is a shadowgram of one of the test models in free flight.

Data Reduction

Data Analysis System

The data analysis system currently in use at the Aeroballistic Research Facility (ARF) is shown graphically in Fig. 5. This system incorporates a standard linear theory analysis and a six-degree-of-freedom (6-DOF) numerical integration technique known as the maximum likelihood method (MLM). At present, three separate 6-DOF packages are available for use in reducing the ballistic range data to coefficient form.

1) MLMFXPL—fixed-plane 6-DOF for symmetric missiles or projectiles including induced forces and moments and aerodynamic trims.

2) MLMBDFX—body-fixed 6-DOF for configurations such as airplanes or symmetric missiles with or without mass asymmetries.

3) MLMBALL—fixed-plane 6-DOF for symmetric missiles or projectiles with moving internal parts such as fuse mechanisms.

Table 1 Physical properties

Shot no.	Mass, g	Length, cm	Diam., cm	$X_{c.g.}/l$	I_x, g-cm^2	I_y, g-cm^2	I_z, g-cm^2
1	177.15	20.875	2.695	0.5174	373.1	6640	6881
2	186.61	20.875	2.685	0.5013	374.0	7028	7272
3	173.49	20.822	2.690	0.5220	371.7	6535	6770

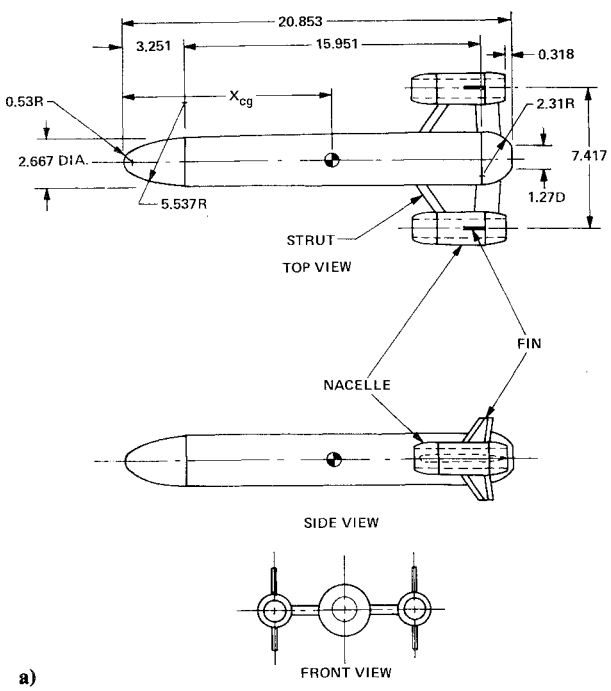

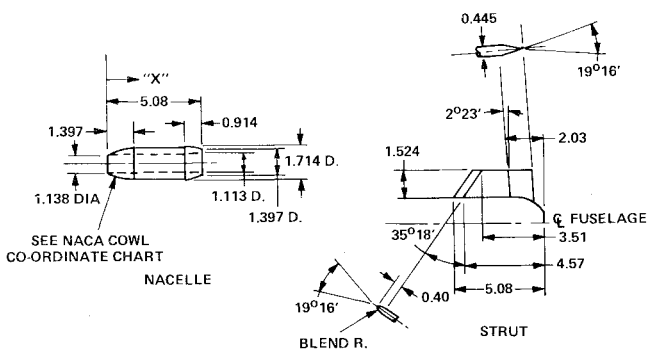

NACA COWL
CO-ORDINATE CHART

"X"	DIA.
0	1.1380
0.0610	1.2930
0.1220	1.3560
0.4240	1.5340
0.6680	1.6180
0.9119	1.6739
1.3970	1.7145

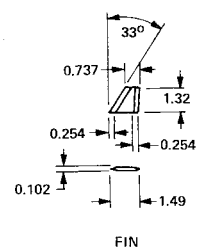

b)

NOTE: ALL DIMENSIONS ARE IN CENTIMETERS UNLESS OTHERWISE NOTED

Fig. 2 Sketch of model configuration.

All 6-DOF programs can reduce up to five experimental sets of data simultaneously and determine the set of aerodynamic coefficients which best fits all the data. The data reduction system has been programmed to operate in a time-sharing interactive mode. Input requirements and initial estimates are kept to a bare minimum. The 6-DOF options require no additional inputs providing that a satisfactory linear theory reduction has been accomplished.

The data presented in this paper utilized the body-fixed 6-DOF program MLMBDFX. The equations of motion contained in the analysis are stated in a following section along with the aerodynamic coefficients model. A brief description of MLM is also presented.

Equations of Motion

Since the aerodynamic forces and moments are defined in a body-fixed coordinate system, the equations of motion were derived with respect to a rotating coordinate system. This coordinate system is defined with the X axis aligned with the longitudinal axis of the missile and points out the nose, the Y axis points out the left wing, and the Z axis points up with respect to the body (see Fig. 1). The body-fixed coordinate system is rigidly attached to the missile and rotates with the missile about the X axis. The inertial frame of reference is the Earth. It is assumed that the Earth is fixed in space and flat. The 6-DOF differential equations derived in this system become (see Ref. 12)

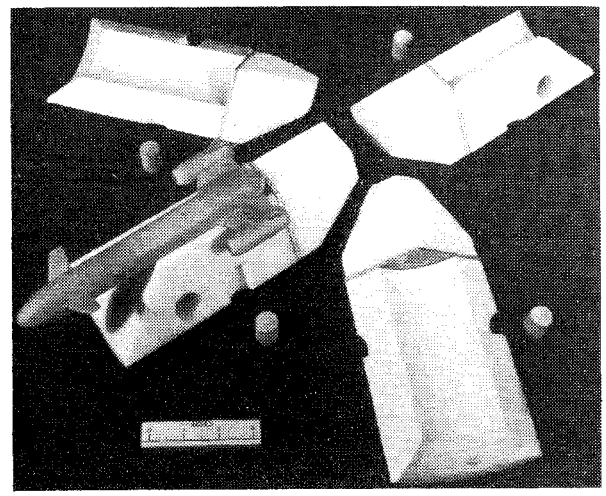

Fig. 3 Photograph of model and sabot package.

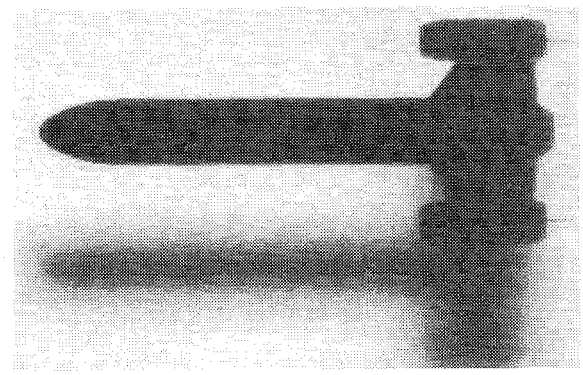

Fig. 4 Typical shadowgram.

$$\dot{u}_b = r_b v_b - q_b w_b - a_{cub} + F_{xb}/m + g\sin\theta \tag{1}$$

$$\dot{v}_b = p_b w_b - r_b u_b - a_{cvb} + F_{yb}/m - g\sin\phi\cos\theta \tag{2}$$

$$\dot{w}_b = q_b u_b - p_b v_b - a_{cwb} + F_{zb}/m - g\cos\phi\cos\theta \tag{3}$$

and

$$\dot{p}_b = \frac{(I_y L_b + I_{xy} M_b - (I_x + I_y - I_z) I_{xy} p_b r_b)}{(I_x I_y - I_{xy}^2)} + \frac{((I_{xy}^2 + I_y (I_y - I_z)) q_b r_b)}{(I_x I_y - I_{xy}^2)} \tag{4}$$

$$\dot{q}_b = \frac{(I_x M_b + I_{xy} L_b + (I_x + I_y - I_z) I_{xy} q_b r_b)}{(I_x I_y - I_{xy}^2)} + \frac{((I_x (I_z - I_x) - I_{xy}^2) p_b r_b)}{(I_x I_y - I_{xy}^2)} \tag{5}$$

$$\dot{r}_b = \frac{N_b + I_{xy}(p_b^2 - q_b^2) + (I_x - I_y) p_b q_b}{I_z} \tag{6}$$

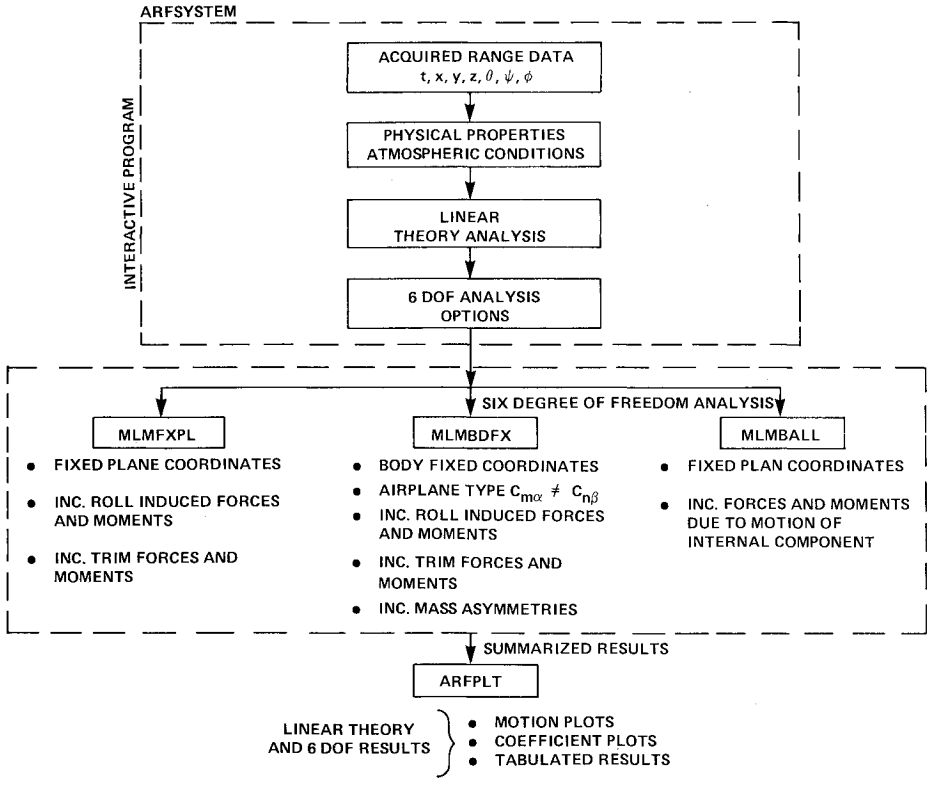

Fig. 5 Aeroballistic Research Facility data analysis system.

Once the definitions of the forces and moments are made, the solution to Eqs. (1-6) will define the 6-DOF flight motion of an asymmetric missile in body-fixed coordinates. Since the position-attitude measurements as acquired from a ballistic spark range are obtained with respect to an Earth-fixed axis system, additional transformation differential equations are required. These transformation equations are expressed below in terms of the body-fixed velocity components (u_b, v_b, w_b, p_b, q_b, and r_b), the fixed-plane Euler angles (θ, ψ), and the angle of rotation about the missile axis (ϕ).

$$\dot{x} = u_b \cos\theta \cos\psi + v_b(\sin\theta \sin\phi \cos\psi - \cos\phi \sin\psi) + w_b(\sin\theta \cos\phi \cos\psi + \sin\phi \sin\psi) \quad (7)$$

$$\dot{y} = u_b \cos\theta \sin\psi + v_b(\sin\theta \sin\phi \sin\psi + \cos\phi \cos\psi) + w_b(\sin\theta \cos\phi \sin\psi - \sin\phi \cos\psi) \quad (8)$$

$$\dot{z} = -u_b \sin\theta + v_b \cos\theta \sin\phi + w_b \cos\theta \cos\phi \quad (9)$$

$$\dot{\theta} = q_b \cos\phi - r_b \sin\phi \quad (10)$$

$$\dot{\psi} = (q_b \sin\phi + r_b \cos\phi)/\cos\theta \quad (11)$$

$$\dot{\phi} = p_b + \tan\theta(q_b \sin\phi + r_b \cos\phi) \quad (12)$$

Coriolis accelerations are also computed and included in Eqs. (1-3).

The preceding equations are numerically integrated using a fourth-order Runge-Kutta scheme. Close attention is paid to the integration time step. A complete derivation of the equations of motion is contained in Ref. 12.

Aerodynamic Model

The primary aerodynamic forces and moments acting on an asymmetric missile in free flight are illustrated in Fig. 1. The forces and moments are a result of the flowfield and associated pressure distributions around a spinning body in free flight. The basic definitions of the aerodynamic forces and moments are shown below and are based on Ref. 12.

$$F_{xb} = \bar{q}A\bar{C}_X \quad (13)$$

$$F_{yb} = \bar{q}A\left(-\bar{C}_{Y0} - \bar{C}_{Y\beta}\frac{v_b}{V} + \bar{C}_{Y\gamma\alpha}\frac{w_b}{V} + \bar{C}_{Yp\bar{\alpha}}\frac{p_b d}{2V}\frac{w_b}{V}\right) \quad (14)$$

$$F_{zb} = \bar{q}A\left(-\bar{C}_{Z0} - \bar{C}_{Z\alpha}\frac{w_b}{V} - \bar{C}_{Y\gamma\alpha}\frac{v_b}{V} - \bar{C}_{Yp\bar{\alpha}}\frac{p_b d}{2V}\frac{v_b}{V}\right) \quad (15)$$

$$L_b = \bar{q}Ad(p_b d/2V \cdot \bar{C}_{lp} + \bar{C}_l) \quad (16)$$

$$M_b = \bar{q}Ad\left(\bar{C}_{m0} + \bar{C}_{m\alpha}\frac{w_b}{V} + \bar{C}_{mq}\frac{q_b d}{2V} + \bar{C}_{np\bar{\alpha}}\frac{p_d d}{2V}\frac{v_b}{V} + \bar{C}_{n\gamma\dot{\bar{\alpha}}}\frac{v_b}{V}\right) \quad (17)$$

$$N_b = \bar{q}Ad\left(-\bar{C}_{n0} - \bar{C}_{n\beta}\frac{v_b}{V} + \bar{C}_{nr}\frac{r_b d}{2V} + \bar{C}_{np\bar{\alpha}}\frac{p_b d}{2V}\frac{w_b}{V} + \bar{C}_{n\gamma\bar{\alpha}}\frac{w_b}{V}\right) \quad (18)$$

The aerodynamic coefficients are assumed to be nonlinear functions of the total angle of attack ($\bar{\alpha}$) or of components of the total angle of attack (α, β). These angles are also defined in Fig. 1. Some of the coefficients are also assumed to be functions of Mach number and the aerodynamic roll angle. The nonlinearities with angle of attack have been modeled as polynomial functions of the sine of the total angle of attack or its components. These coefficient expansions are shown below:

$$\bar{C}_X = C_{X0} + C_{X\alpha 2}(w_b/V)^2 + C_{X\beta 2}(v_b/V)^2 + C_{Xm}(m_i - m_0) + C_{X\bar{\alpha}2}\epsilon^2 \quad (19)$$

$$\bar{C}_{Y0} = C_{Y0} \quad (20)$$

$$\bar{C}_{Z0} = C_{Z0} \tag{21}$$

$$\bar{C}_{Y\beta} = C_{Y\beta} + C_{Y\beta 3}(v_b/V)^2 + C_{Z\bar{\alpha}} + C_{Z\bar{\alpha}3}\epsilon^2 + C_{Z\gamma\bar{\alpha}3}\epsilon^2 \cos N\gamma \tag{22}$$

$$\bar{C}_{Z\alpha} = C_{Z\alpha} + C_{Z\alpha 3}(w_b/V)^2 + C_{Z\bar{\alpha}} + C_{Z\bar{\alpha}3}\epsilon^2 + C_{Z\gamma\bar{\alpha}3}\epsilon^2 \cos N\gamma \tag{23}$$

$$\bar{C}_{Y\gamma\bar{\alpha}} = C_{Y\gamma\bar{\alpha}3}\epsilon^2 \sin N\gamma \tag{24}$$

$$\bar{C}_{Yp\bar{\alpha}} = C_{Yp\bar{\alpha}} \tag{25}$$

$$\bar{C}_{lp} = C_{lp} \tag{26}$$

$$\bar{C}_l = C_{l\delta}\delta + C_{l\gamma\alpha 2}\epsilon^2 \sin N\gamma \tag{27}$$

$$\bar{C}_{m0} = C_{m0} \tag{28}$$

$$\bar{C}_{n0} = C_{n0} \tag{29}$$

$$\bar{C}_{m\alpha} = C_{m\alpha} + C_{m\alpha 3}(w_b/V)^2 + C_{m\bar{\alpha}} + C_{m\bar{\alpha}3}\epsilon^2 + C_{m\gamma\bar{\alpha}3}\epsilon^2 \cos N\gamma + \bar{C}_{z\alpha}(CG - CG_0) \tag{30}$$

$$\bar{C}_{mq} = C_{mq} + C_{mq\alpha 2}(w_b/V)^2 + C_{m\dot{\bar{q}}} + C_{m\dot{\bar{q}}\bar{\alpha}2}\epsilon^2 \tag{31}$$

$$\bar{C}_{n\beta} = C_{n\beta} + C_{n\beta 3}(v_b/V)^2 + \bar{C}_{m\bar{\alpha}} + C_{m\bar{\alpha}3}\epsilon^2 + C_{m\gamma\bar{\alpha}3}\epsilon^2 \cos N\gamma + \bar{C}_{y\beta}(CG - CG_0) \tag{32}$$

$$\bar{C}_{nr} = C_{nr} + C_{nr\beta 2}(v_b/V)^2 + C_{m\dot{\bar{q}}} + C_{m\dot{\bar{q}}\bar{\alpha}2}\epsilon^2 \tag{33}$$

$$\bar{C}_{n\gamma\bar{\alpha}} = C_{n\gamma\bar{\alpha}3}\epsilon^2 \sin N\gamma \tag{34}$$

$$\bar{C}_{np\bar{\alpha}} = C_{np\bar{\alpha}} \tag{35}$$

The aerodynamic roll angle is computed as follows:

$$\gamma = \tan^{-1}(v_b/w_b) \tag{36}$$

The authors are aware that the sine-cosine expansions of the induced terms are ideal and higher order effects have been observed during some wind tunnel tests at large angles of attack ($\bar{\alpha} > 10$ deg). However, in the absence of a higher-order theory, the ideal model was utilized.

Maximum Likelihood Method

The maximum likelihood method is a technique which can be used to match a theoretical trajectory to one observed experimentally. As used in the present routines, it is an iterative procedure which adjusts the aerodynamic coefficients to maximize a likelihood function. The essential steps of the analysis are briefly summarized. The equations of motion are derived containing all of the necessary aerodynamic coefficients. By numerically integrating the equations of motion, the theoretical trajectory is obtained. The actual trajectory is known from the experimental measurements. The gist of the method is to adjust the aerodynamic coefficients contained in the equations of motion in such a way that the so-obtained trajectory matches the measurements. The mathematical treatment is a sensitivity analysis. The sensitivity equations or partial differential equations form a basis for the method of quasiilinearization and are derived by formally differentiating the equations of motion with respect to the coefficients. The sensitivity equations are integrated in parallel with the equations of motion to yield sensitivity coefficients (partial derivatives), which reflect the sensitivity of the computed solution with respect to each aerodynamic coefficient or system parameter (e.g. initial condition).

The use of a truncated Taylor series expansion brings about a method of quasilinearization which uses these sensitivity coefficients to linearize the change in the solution of the nonlinear equations of motion due to a change in the aerodynamic coefficients or system parameters. In other words, the Taylor series expansion forms a relationship between residuals (computed vs experimental), correction to the coefficients, and the partial derivatives. This is illustrated as follows:

$$\sum^{N} [R] = \sum^{N} [E] - \sum^{N} [A][\Delta C] \tag{37}$$

where N is the number of data points, $[E]$ the residual matrix from 6-DOF motion (x, y, z, θ, ψ, ϕ), $[\Delta C]$ the matrix of corrections to be made to the aerodynamic coefficients and system parameters, $[A]$ the partial derivative matrix of the six degree-of-freedom with respect to the coefficients, and $[R]$ represents the residuals after the corrections have been made as the theoretical trajectory is matched to the actual. In an iterative sense, $[R]$ is one iteration ahead of $[E]$. In the limit, as convergence is achieved, $[E]$ should approach $[R]$ as being a measure or the experimental errors of measurement noise.

This technique has become known as differential corrections. It should be noted that the elements of the $[A]$ matrix are obtained from the integration of their derivatives with respect to time.

The maximum likelihood method is an iterative procedure which adjusts the aerodynamic coefficients to maximize a likelihood function, thereby matching the theoretical trajectory to the actual. The function is expressed as follows:

$$L = \frac{1}{(2\pi)^{1/2}|[S]|^{1/2}} \exp\left(\frac{-1}{2} \sum^{N} [R]^T [S]^{-1} [R]\right) \tag{38}$$

where $[S]$ is the covariance matrix of the measurement noise. Its application to data correlation eliminates the inherent assumption in least-squares theory where the magnitude of the measurement noise must be consistent between dynamic parameters (irrespective of units). This is achieved through the use of the covariance matrix which contains statistical information concerning the measurement noise of each dynamic parameter (6-DOF). The likelihood function also has the property of asymptotically approaching the correct solution as opposed to parabolically with least squares. The use of this method allows simultaneous correlation of all six degrees-of-freedom to determine the aerodynamic force and moment coefficients. For the application discussed herein, the values of the measurement noise contained in the covariance matrix were chosen by the experience gained from analyzing the flights of hundreds of models tested within the Aeroballistic Research Facility.

Results and Discussion

The flights of the three models flown in order to demonstrate the data reduction procedures were analyzed using the equations of motion and the aerodynamic model previously discussed. Shadowgrams (dual plane) were obtained for 12 locations covering approximately 50 m in range for each shot. The shadowgrams were read on a high-quality film reader. From the film readings and timing station data, a time-based trajectory is constructed (t, x, y, z, θ, ψ, ϕ). This data is then coupled with the measured physical properties and submitted to data analysis. These flights were initially analyzed separately but ultimately were simultaneously analyzed (multiple fit) such that a common set of aerodynamics was determined that best matched each of the separately measured position-attitude-time profiles. Using this multiple fit method, a more complete range of angle of attack and roll orientation combinations are available for analysis than would be available for each of the flights considered separately. This increases the probability that the determined coefficients define the model aerodynamics over the entire

range of possible angles of attack and roll combinations. The results discussed in this paper were obtained using this multiple fit reduction. These multiple fitting techniques are outlined in Ref. 13.

The position and attitude measurements for each of the three flights are shown in Figs. 6-8 along with the theoretically fitted motions. These plots show that the previously discussed mathematical model and the maximum likelihood method of fitting adequately matches the experimentally measured motion profiles. In fact the probable errors of the combined fits approach the measurement capabilities of the facility for this configuration (see Table 2).

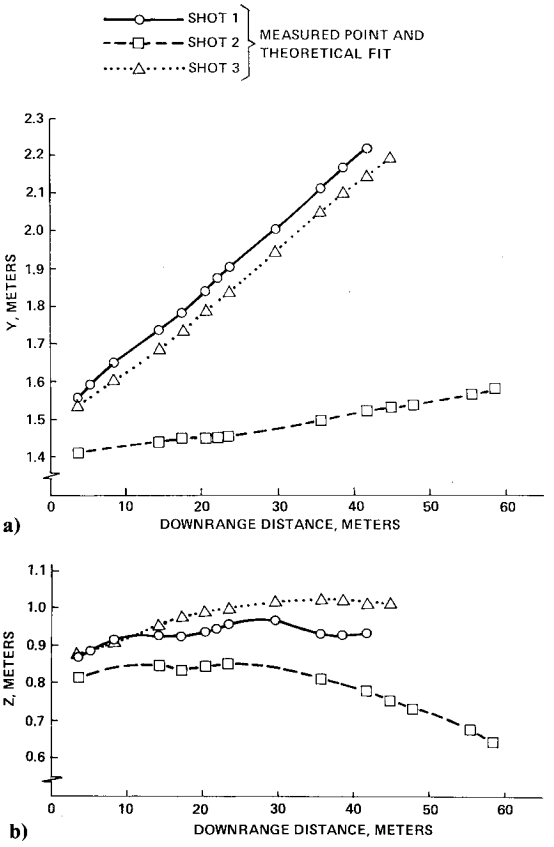

Fig. 6 Motion of the model's center of gravity: a) crossrange, b) vertical.

When viewing the results of Table 2 and the motion plots of Figs. 6-8, it should be noted that the theoretical fits for each of the three flights are defined by a common set of aerodynamic coefficients. The coefficients that were determined, along with the associated probable errors, are tabulated in Table 3.

The aerodynamic coefficients shown in Table 3 represent a unique solution within the limitations of the motion profiles (translational and angular) observed during these three shots. Considering the 12 measurement stations for each shot, there is a total of 36 sets (t, x, y, z, θ, ψ, ϕ) of dynamic data matched simultaneously to the coefficients in Table 3. To initialize the 6-DOF data analysis, estimates of $C_{m\alpha}$, $C_{n\beta}$, C_{mq}, C_{nr}, C_{X0}, $C_{Z\alpha}$, $C_{Y\beta}$, and C_{lp} were provided as determined by the linear theory analysis. Subsequently to obtaining a best fit to the data using the linear aerodynamic coefficients,

Table 2 Precision of fit

	θ,ψ, deg	ϕ, deg	X, m	Y,Z, m
Probable error of fit	0.189	2.80	0.00150	0.00065
Facility measurement capability	0.100	1.00	0.00075	0.00030

Table 3 Aerodynamic results

Coefficient	Determined value of coefficient	Associated probable error
$C_{m\alpha}$	−22.97	0.29
$C_{n\beta}$	−10.50	0.11
C_{mq}	−241.9	16.3
C_{nr}	−31.2	7.4
$C_{n\gamma\hat{\alpha}3}$	−149.2	24.0
$C_{m\gamma\hat{\alpha}3}$	−45.0	6.4
C_{X0}	0.491	0.006
$C_{X\alpha 2}$	−20.4	6.9
$C_{X\beta 2}$	0.70	0.84
$C_{Z\alpha}$	16.14	0.65
$C_{Y\beta}$	7.76	0.21
C_{lp}	−7.72	1.68
$C_{l\gamma\hat{\alpha}2}$	−0.88	0.62

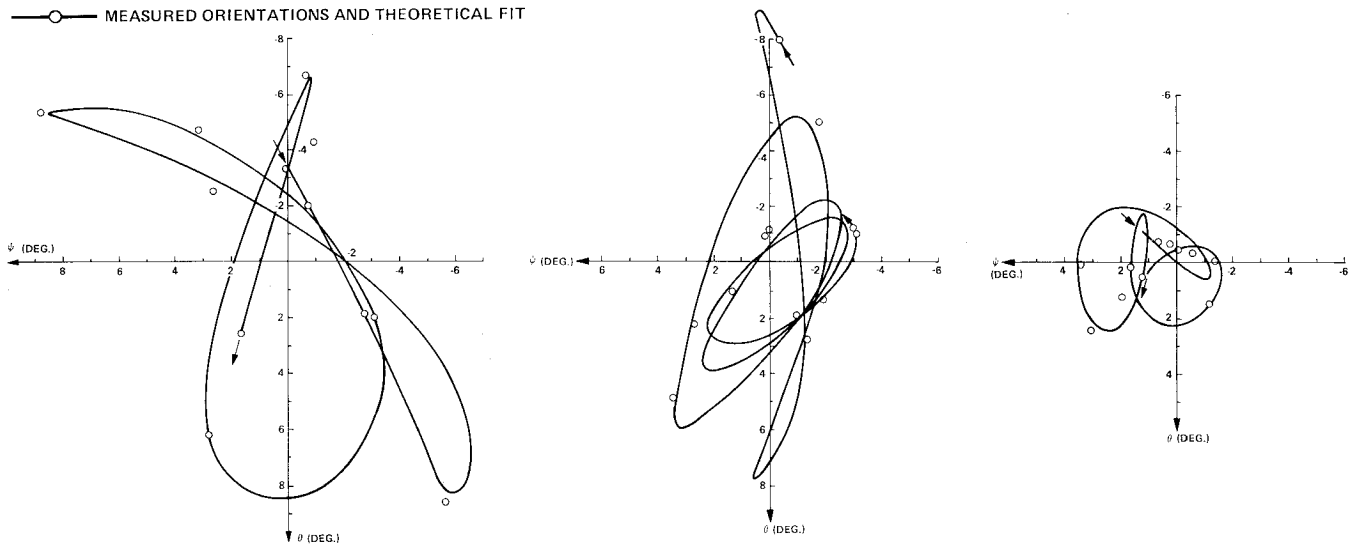

Fig. 7 Fixed-plane angular motions for shot 1 (left), shot 2 (center), and shot 3 (right).

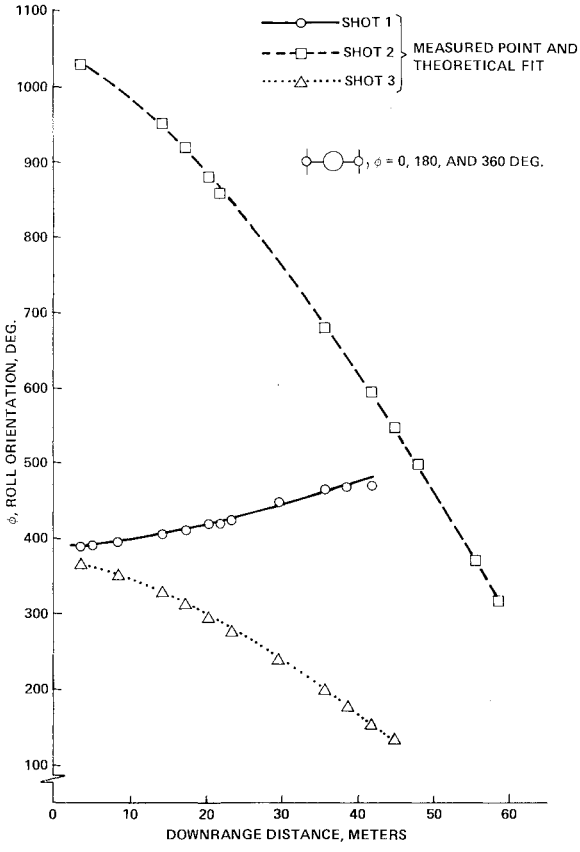

Fig. 8 Rolling motions.

the higher-order coefficients were determined. Wind tunnel data on this configuration does not exist. If the aerodynamics in Table 3 were used in a 6 DOF trajectory simulation, the motion observed during these ballistic range flights would be duplicated. A comparison of free-flight and wind-tunnel aerodynamic results on a research missile configuration is contained in Ref. 10.

The results shown in Table 3 indicate that the static ($C_{m\alpha}$ and $C_{n\beta}$) and dynamic stability (C_{mq} and C_{nr}) differed appreciably in the pitch and yaw plane. The ratio of the pitch force derivative ($C_{Z\alpha}$) and the side force derivative ($C_{Y\beta}$) is consistent with the ratio of $C_{m\alpha}$ and $C_{n\beta}$. These coefficients are accurately determined as indicated by their associated probable errors. The roll-induced side moment ($C_{n\gamma\bar{\alpha}3}$) is significantly larger than the roll-induced pitching moment ($C_{m\gamma\bar{\alpha}3}$), which is in agreement with the results of Ref. 10. Although the zero-angle-of-attack axial force coefficient (C_{X0}) is very well determined, the effects on C_X caused by pitch and yaw ($C_{X\alpha 2}$ and $C_{X\beta 2}$) appear questionable. This is probably due to the fact that relatively small angles of attack were experienced during the flights; therefore, these derivatives did not measurably affect the resulting motions. Likewise, the determined roll damping derivative (C_{lp}) is reasonable, but the induced roll moment ($C_{l\gamma\bar{\alpha}2}$) was not adequately determined. The effect of $C_{l\gamma\bar{\alpha}2}$ on the measured rolling motions was too small to determine this derivative.

There are many more coefficients and higher-order derivatives shown in the aerodynamic expansions previously discussed than were determined and tabulated in Table 3. Several additional computer runs were accomplished in an attempt to determine some of these higher-order coefficients. However, even though the probable errors of fit may have slightly decreased from those shown in Table 2, the probable error associated with the determined higher-order coefficient was excessively large. This conclusion was not unexpected since it is unreasonable to assume that all of the aerodynamic coefficients and their higher-order terms can be determined from each set of position-attitude-time measurements. It is expected and believed demonstrated that those coefficients which measurably affect the experimental motion profiles have been determined. The results shown in Table 3 demonstrate that the asymmetric aerodynamics have been successfully extracted from the measured motions of this complex missile configuration.

Concluding Remarks

It has been demonstrated that asymmetric missile configurations can be routinely tested and the aerodynamics extracted from free-flight ballistic range measurements using the maximum likelihood method. The authors of this paper do not claim that the equations of motion or the functional forms of the aerodynamic model used within the present routines will be sufficient for all possible test configurations. These can and will be altered as required on an individual basis; however, the present formulation adequately matched the measured motion profiles of the configuration chosen for this demonstration. This analysis technique considerably expands the capabilities of ballistic ranges and provides the test engineer with additional testing options. No longer should free-flight ranges be considered solely for testing symmetrical configurations.

References

[1] Murphy, C.H., "Data Reduction for the Free Flight Spark Ranges," Ballistic Research Lab., Aberdeen Proving Ground, Rept. 900, Feb. 1954.

[2] Murphy, C.H., "Free Flight Motion of Symmetric Missiles," Ballistic Research Lab., Aberdeen Proving Ground, Rept. 1216, July 1963.

[3] Murphy, C.H., "The Measurement of Non-Linear Forces and Moments by Means of Free Flight Tests," Ballistic Research Lab., Aberdeen Proving Ground, Rept. 974, Feb. 1956.

[4] Krial, K.S. and MacAllister, L.C., "Aerodynamic Properties of a Family of Shells of Similar Shape – 105 mm, XM380E5, XM389E6, T388 and 155 mm T387," Ballistic Research Lab., Aberdeen Proving Ground, MR2023, Feb. 1970.

[5] Nicolaides, J.D. and MacAllister, L.C., "A Review of Aeroballistic Range Research on Winged and/or Finned Missile," Ballistic TN No. 5, Bureau of Ordinance, Dept. of Navy, 1955.

[6] Nicolaides, J.D., "Free Flight Dynamics," University of Notre Dame, South Bend, Ind., 1967.

[7] Nicolaides, J.D., "On the Free Flight Motion of Missiles Having Slight Configurational Asymmetrics," Ballistic Research Lab., Aberdeen Proving Ground, Rept. 858, June 1953.

[8] Eikenberry, R.S., "Analysis of the angular Motion of Missiles," University of Notre Dame, Sandia Rept. SC-CR-70-6051, Feb. 1970.

[9] Chapman, G.T. and Kirk, D.B., "A Method for Extracting Aerodynamic Coefficients from free Flight Data," *AIAA Journal*, Vol. 8, April 1970, pp. 753-757.

[10] West, K.O. and Whyte, R.H., "Free Flight and Wind Tunnel Test of a Missile Configuration at Subsonic and Transonic Mach Numbers with Angles of Attack up to 30 Degrees," Paper 39, 11th Navy Symposium on Aeroballistics, Trevose, Penn., Aug. 1978.

[11] Winchenbach, G.L., Galanos, D.G., Kleist, J.S., and Lucas, B.F., "Description and Capabilities of the Aeroballistics Research Facility," AFATL-TR-78-14, April 1978.

[12] Hathaway, W.H. and Whyte, R.H., "Aeroballistic Range Data Analysis for Nonsymmetric Configurations," AFATL-TR-76-109, Sept. 1976.

[13] Whyte, R.H. and Hathaway, W.H., "Aeroballistic Range Data Reduction Technique Utilizing Numerical Integration," AFATL-TR-74-41, Feb. 1974.